GEOPHYSICAL FIELD INVESTIGATION OF A POTENTIAL HYPER-ARID DESERT ANALOG TO MARS: THE WESTERN DESERT OF EGYPT. C. L. Dinwiddie[1], S. K. Sandberg[2], R. N. McGinnis[1], and R. E. Grimm[3], [1]Department of Earth, Material, and Planetary Sciences, Southwest Research Institute®, 6220 Culebra Road, San Antonio, TX 78238 (cdinwiddie@swri.org), [2]116 Sycamore St. NE, №.6, Albuquerque, NM 87106, [3]Department of Space Studies, Southwest Research Institute®, 1050 Walnut St., №.400, Boulder CO 80302.

Introduction: We are evaluating the performance potential of low-frequency (12.5–100 MHz) ground-penetrating radar (GPR) and other geophysical methods for subsurface investigation of Mars. Our search for terrestrial analog sites began with the understanding that sites best suited for this work should be sufficiently characterized to provide an accurate understanding of the local *geologic* context. Initial studies, however, resulted in a newfound appreciation for the importance of geophysical characterization to attain an accurate understanding of the local *geoelectrical* context [1]. If the geoelectrical character of the subsurface is not sufficiently analogous to that hypothesized for Mars, the performance of low-frequency radar may be moderate, at best. Thus, in an effort to identify suitable analogs to Mars, we are conducting transient electromagnetic (TEM) and vertical electrical soundings (VES) of potential analog sites to quantify the geoelectrical characteristics of the subsurface. This paper summarizes our recent work in the western desert of Egypt.

Motivation and Field Methods: The NetLander radar team conducted a ground-penetrating radar survey (0.5–5 MHz) in the western desert of Egypt in March 2003. Electromagnetic properties of samples available from the land surface were measured in the laboratory to construct a geoelectrical profile in support of this initial investigation [2]. Survey results suggested that background athropogenic noise (e.g., from communication) is extremely low in this remote region, which is a favorable Mars analog condition for radar soundings. Results also suggested that ambiguities associated with discrimination between lithologic and hydrologic interfaces or the presence of surface multiples in a wiggle trace could be reduced through the acquisition of TEM and VES data.

TEM. Transient electromagnetic soundings are performed to provide information about the electrical resistivity of subsurface units. A central loop TEM sounding configuration was used, whereby a wire loop at the ground surface transmits a primary electrical current, which induces a primary, steady-state magnetic field in the subsurface. The transmitted current is abruptly terminated at the surface, causing the primary magnetic field to decay with time. Secondary currents in the subsurface induced by the decaying primary magnetic field propagate downward and outward, generating a transient secondary magnetic field. The voltage or current flow induced in a wire receiver coil at the ground surface by the time-varying secondary magnetic field is recorded. Early time samples of the decay relate to shallow currents flowing near the transmitter loop, and late time samples of the decay relate to deeper subsurface currents. Magnetic field decay data are inverted using a numerical formulation to determine the distribution of resistivity with depth. TEM data were acquired using both a low power transmitter that supports relatively small loop geometries (e.g., 40 × 40 m), which is best suited for mapping relatively shallow conductive structures (i.e., generally ~40 m), and a high power transmitter that supports large loop geometries (e.g., 300 × 300 m) and is, therefore, capable of mapping structures several hundred meters deep.

VES. Vertical electrical soundings using the four-electrode collinear symmetric Schlumberger array can also be performed to determine the electrical resistivity of near-surface units, but with a resolution that exceeds that of TEM. Current is injected directly into the subsurface between two outer electrodes and the potential is measured between two inner electrodes. The resistivity of the subsurface is measured as a function of depth by expanding the current electrodes about a central stationary point. Because of the geometric configuration of the Schlumberger array, the resolution capabilities of the method are generally limited to the near surface. As a result, the method is primarily deployed for mapping the resistivity structure down to a depth of a few tens of meters.

Simultaneous Inversion. Subsurface electrical resistivity is determined by inverting TEM and VES data. These data may be inverted either independently or simultaneously using the computer program EINVRT6 [3,4]. EINVRT6 is a one-dimensional discrete layered-resistivity software package that uses a non-linear least squares inverse solution to determine resistivity and thickness of each model layer. Modeling nonuniqueness makes identification of the best resistivity model for a given dataset (e.g., VES data) at a field site difficult (i.e., a range of subsurface resistivity configurations may yield a similar voltage response at the ground surface). To reduce model nonuniqueness and better constrain model parameters, simultaneous inversion of information from a second independent source or multiple independent sources can be used.

Data Collection: We performed TEM and VES soundings in the hyper-arid (annual average precipitation ≤5 mm/yr) western desert of Egypt in November 2005. Our study site comprises three locations oriented in an east-west profile spanning 4.8 km on the 10-km-wide El-Quss Abu Sa'id plateau. This plateau is more than 250 m higher than the Farafra Oasis basin and is located 18 km from the oasis along a bearing of 305°. These locations were characterized to capture both vertical and lateral variations in subsurface resistivity structure.

Site Description: Site stratigraphy is composed of lower Eocene and Paleocene sedimentary units. The plateau at the sounding location is capped by the lower Eocene-age Farafra formation. These units are composed of a 5–25-m-thick white alveolinid limestone overlying a 25-m-thick dark yellow nummulite limestone. The marine limestones of the Farafra formation transition into the coeval Dungul formation, which is composed of a ~100-m-thick marly limestone and evaporite sequence interbedded with shales and clays. The Paleocene-age rocks of the Esna shale and Garra formation underlie the lower Eocene units and consist of 100-m-thick green shale that transitions at depth into alternating beds of shale and limestone. [5]

Upper Cretaceous-aged rocks of the Dahkla and Nubia formations lie below the plateau-forming units. The Dahkla formation, exposed at the surface of the Farafra Oasis, is composed of interbedded shale, limestone, clay, and sandstone layers. [5] The Nubia Formation underlies the Dahkla and contains the major water-supply aquifer for two major sedimentary basins in this region. The Dakhla Basin of Egypt and the Kufra Basin of Libya form a regional aquifer system with an area of ~2×10^6 km^2 [6,7]. The principal water-bearing formation below the field site is the 2000-m-thick Nubian Sandstone [8]. Where the aquifer deepens to the north, it is overlain with sand and pre-Tertiary marine sedimentary rock consisting of dry porous dolomite, clay, and gravel [7,9]. The aquifer is located in the lower section of the Nubian Sandstone where it is confined beneath low permeability clay.

Results: Simultaneous inversions of TEM and VES data produced geoelectrical models that are consistent with the known geology and hydrogeology. At the eastern end of the 4.8 km profile, the lower Eocene-aged unit extends to a depth of ~60 m. This unit has a bulk resistivity ranging from 5.4 to 2700 Ω·m. High resistivities are found exclusively in the dessicated near-surface section. From 60 to >200 m depth, the Paleocene-age unit is mapped as a geoelectrical conductor with a bulk resistivity of 1.9 Ω·m (Fig. 1). At >200 m depth, and at the extreme limits of detection for the geophysical arrays used, a more resistive unit is modeled with bulk resistivity greater than that of the overlying shale, but with a poorly resolved value. Based upon correlation with known hydrogeology, lithology, and elevation, we interpret this underlying resistive layer to represent the water-bearing unit of the Nubia Formation.

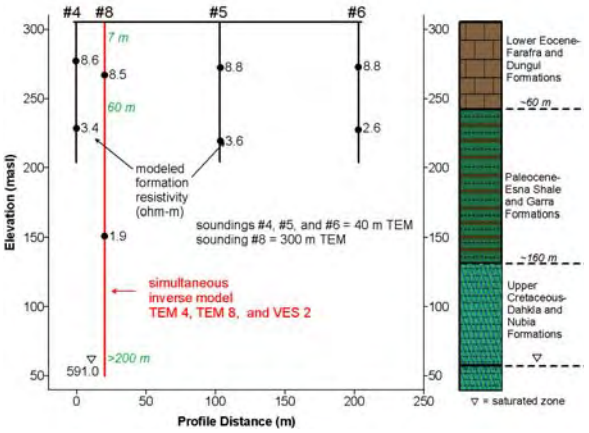

Fig. 1. Resistivity cross-section for eastern end of 4.8 km profile.

Three 40-m-loop TEM soundings at 100 m spacings (Fig. 1) were independently inverted to investigate geoelectrical heterogeneity where lithology appeared generally homogeneous. These geophysical data indicate minor lateral and vertical facies variation with enhancement of electrical conductivity in the upper part of the Paleocene-aged unit at ~60 m depth and toward the southeast. This result is consistent with natural variability in this depositional environment.

Conclusions: Simultaneous inversion of TEM and VES data is an appropriate technique for resolving ambiguities associated with GPR identification of lithologic and hydrologic interfaces in the subsurface and for quantifying radar signal attenuation. An integrated interpretation of radar and resistivity data collected along our profile in November 2005 will be presented at *LPSC XXXVII* [10,11]. Preliminary results indicate radar attenuation may be problematic because of residual salinity in these marine units where clays trap concentrated salt solutions, not withstanding the hyper-aridity of the modern climate in this region.

References: [1] Dinwiddie C. L. et al. (2005) *Workshop on Radar Investigations of Planetary and Terrestrial Environments*, Abstract #6035. [2] Jernsletten J. A. and Heggy E. (2004) *LPSC XXXV*, Abstract #2089. [3] Sandberg S. K. (1990) New Jersey Geological Survey Open-File Report OFR90-1. [4] Sandberg S. K. (1993) *Geophysical Prospecting*, *41*, 207–227 [5] Egyptian Geological Survey and Mining Authority (1982) *Dakhla Geological Map Sheet NG-35*. [6] Schneider M. (1986) *Berliner Geowiss. Abh.*, *71*, 1–66. [7] Hesse K. H. et al. (1987) *Berliner Geowiss. Abh.*, *75*, 397–464. [8] Egyptian Survey Authority (1999) *Hydrogeological Map of Egypt*, 2nd ed. [9] Shata A. A. (1982) *Quarterly J. Eng. Geol. & Hydrogeol.*, *15*, 127–133. [10] Clifford S. M. et al. (2006) these abstracts. [11] Ciarletti V. et al. (2006) these abstracts.